

## Electrochemistry of Oxygen in Concentrated NaOH Solutions: Solubility, Diffusion Coefficients, and Superoxide Formation

Cunzhong Zhang,<sup>†</sup> Fu-Ren F. Fan, and Allen J. Bard\*

Center for Electrochemistry, Department of Chemistry and Biochemistry, The University of Texas at Austin, Austin, Texas 78712-0165

Received August 13, 2008; E-mail: ajbard@mail.utexas.edu

**Abstract:** The diffusion coefficient ( $D_{O_2}$ ), solubility ( $C_{O_2}$ ), and electrochemical behavior of oxygen reduction were investigated by cyclic voltammetry and transient amperometry on a Pt ultramicroelectrode in aqueous solutions containing various concentrations of NaOH (1–12 M). The results show that both  $D_{O_2}$  and  $C_{O_2}$  decrease as the solution viscosity ( $\eta$ ) increases significantly with increasing concentration of NaOH. The Stokes–Einstein relationship ( $D_{O_2}$  vs  $1/\eta$ ) is followed, yielding a radius for the  $O_2$  molecule, 2.8 Å, that does not change over the concentration range of NaOH studied. From results reported previously for  $C_{O_2}$  in more dilute NaOH solutions and the new results here, the number of electrons,  $n$ , involved in the first step of the oxygen reduction reaction (ORR) was found to change with the concentration of NaOH, from  $n = 2$  at low NaOH concentrations (1–2 M) to  $n = 1$  at high concentrations (>6 M), in line with the changing water activity. Scanning electrochemical microscopy (SECM) was employed as a sensitive tool to investigate the electrochemical behavior of the product of the ORR in 10 M NaOH solution,  $O_2^{\bullet-}$ , as a function of potential. The SECM approach curves depend on the substrate bias and state of the Pt substrate surface, and the apparent rate constant for the redox couple of  $O_2/O_2^{\bullet-}$  is determined to be about  $2.6 \times 10^{-4}$  cm/s in this solution.

### Introduction

The properties and reactions of oxygen are among the most important in chemistry. For example, the oxygen reduction reaction (ORR) and the products of the reaction as a function of the solution environment are active research areas for both practical applications, such as in fuel cells and biological systems, and fundamental studies.<sup>1–4</sup> The mechanism of the ORR is strongly affected by electrolytic environment and, in electrochemistry, the nature of the electrode material.<sup>5</sup> For example, one-electron quasi-reversible electroreduction of  $O_2$  to superoxide ion is observed in aprotic solvents,<sup>6–10</sup> while two-electron (to peroxide) or four-electron (to water) electroreduction is generally found with aqueous electrolytes.<sup>11,12</sup> Superoxide

ion is also often proposed as an intermediate in the ORR<sup>13</sup> and has been found in 1 M KOH at a methylphenyl-modified carbon electrode.<sup>14</sup> Surprisingly, the behavior of  $O_2$  in very concentrated alkaline solutions has not been reported, perhaps because of difficulties with studies in such media.<sup>15</sup> For example, even the solubility of  $O_2$  in >7 M NaOH has not been previously reported. The lifetime of  $O_2^{\bullet-}$  is strongly affected by the rates of its disproportionation and protonation reactions,<sup>16–18</sup> and generally  $O_2^{\bullet-}$  as a dissolved free ion is not obtained easily in aqueous solutions. However, superoxide can be produced by pulse radiolysis in aqueous solution.<sup>19–21</sup>

In aqueous electrolytes, the relationship among  $O_2$ ,  $O_2^{\bullet-}$ , and  $OH^-$  is described by the following chemical reaction:



Thermodynamic data<sup>22</sup> indicate that this reaction has an equilibrium constant of about  $10^3$  and probably proceeds by an

<sup>†</sup> On leave from Beijing Key Laboratory of Environmental Science and Engineering, Beijing Institute of Technology, Beijing, 100081, China.

- (1) Adzic, R. In *Electrocatalysis*; Lipkowsky, J., Ross, P. N., Eds.; Wiley-VCH: New York, 1998.
- (2) Markovi, N. M.; Gasteiger, H. A.; Ross, P. N. *J. Phys. Chem.* **1995**, *99*, 3411.
- (3) Petlicki, J.; van de Ven, T. G. M. *J. Chem. Soc., Faraday Trans.* **1998**, *94*, 2763.
- (4) Liu, B.; Bard, A. J. *J. Phys. Chem. B* **2002**, *106*, 12801.
- (5) Sawyer, D. T., Jr.; Angells, C. T., Jr.; Tsuchiya, T. *Anal. Chem.* **1982**, *54*, 1720.
- (6) Johnson, E. L.; Pool, K. H.; Hamm, R. E. *Anal. Chem.* **1966**, *38*, 183.
- (7) Peover, M. E.; White, B. S. *Chem. Commun.* **1965**, 183.
- (8) Maricle, D. L.; Hodgson, W. G. *Anal. Chem.* **1965**, *37*, 1562.
- (9) Ortiz, M. E.; Núñez-Vergara, L. J.; Squella, J. A. *J. Electroanal. Chem.* **2003**, *549*, 157.
- (10) Vasudevan, D.; Wendt, H. J. *Electroanal. Chem.* **1995**, *192*, 69.
- (11) Bard, A. J.; Stratmann, M. In *Inorganic Electrochemistry*; Scholz, F., Pickett, C. J., Eds.; Encyclopedia of Electrochemistry Vol. 7a; Wiley-VCH: Weinheim, 2006; Chap. 5, p119.
- (12) Shi, C.; Anson, F. C. *Inorg. Chem.* **1998**, *37*, 1037.

- (13) Shao, M.-H.; Liu, P.; Adzic, R. R. *J. Am. Chem. Soc.* **2006**, *128*, 7408, and references therein.
- (14) Yang, H.-H.; McCreery, R. L. *J. Electrochem. Soc.* **2000**, *147*, 3420.
- (15) Licht, S. In *Electroanalytical Chemistry*; Bard, A. J., Rubinstein, I., Eds.; Marcel Dekker: New York, 1998; Vol. 20, p 87.
- (16) Saveant, J.-M. *J. Phys. Chem. C* **2007**, *111*, 2819.
- (17) Sawyer, D. T.; Valentine, J. S. *Acc. Chem. Res.* **1981**, *14*, 393.
- (18) Che, Y.; Tsushima, M.; Matsumoto, F.; Okajima, T.; Tokuda, K.; Ohsaka, T. *J. Phys. Chem.* **1996**, *100*, 20134.
- (19) Czapski, G.; Dorfman, L. M. *J. Phys. Chem.* **1964**, *68*, 1169.
- (20) Saito, E.; Bielski, B. H. J. *J. Am. Chem. Soc.* **1961**, *83*, 4467.
- (21) Kroh, J.; Green, B. C.; Spinks, J. W. T. *J. Am. Chem. Soc.* **1961**, *83*, 2201.
- (22) Conway, B. E.; Bockris, J. O.; Yeager, E.; Khan, S. U. M.; White, R. E. *Comprehensive Treatise of Electrochemistry*; Plenum Press: New York, 1983; Vol. 7, p 301.

initial protonation of  $O_2^{*-}$ .<sup>14</sup> Thus, high concentrations of  $OH^-$  promote the existence of  $O_2^{*-}$  in aqueous solution. Studies of the effect of acidity on the ORR have largely focused on aprotic electrolytes.<sup>23,24</sup> We explore here these processes in aqueous solution under strongly alkaline conditions.

Besides the effect of electrolytes mentioned above, the electrode materials also play an important role. For example, Pt is widely used in practical applications of the ORR reaction and is said to adsorb  $O_2^{*-}$  and to promote the 4e path. We know of no electrochemical studies in aqueous solutions that showed  $O_2^{*-}$  production directly at a Pt electrode, as we find in the present work. We have investigated the ORR by cyclic voltammetry (CV), potential step chronoamperometry at an ultramicroelectrode (UME),<sup>25</sup> and scanning electrochemical microscopy (SECM)<sup>26</sup> and report new results on  $O_2$  solubility, diffusion coefficient, and the heterogeneous rate constant for  $O_2^{*-}$  formation.

## Experimental Section

**Chemicals.** NaOH (ACS reagent grade) was dissolved in Milli-Q water to make a series of concentrations of NaOH aqueous solution, from 1 to 12 M. NaOH solutions, saturated with either highly pure Ar or  $O_2$ , were employed as the blank or working solution, respectively.

**Techniques and Apparatus.** All electrochemical measurements were carried out on a CHI model 660 electrochemical workstation or a CHI 900 SECM system (CH Instruments, Austin, TX) at  $296 \pm 0.5$  K. A large-area Ti screw was used as the counter electrode. A HgO/Hg (14 M NaOH) electrode, placed within a Luggin capillary, was used as the reference electrode (0.006 V vs SHE). A Pt disk UME was constructed by sealing Pt wire in borosilicate glass, with a Pt disk diameter of 25  $\mu\text{m}$  and RG (the ratio of total radius of the tip to radius of the Pt disk) of 3.5, and was used as a working electrode or SECM tip. It is known that strongly alkaline solutions can etch glass, and we were concerned that, upon exposure to our test solutions, the electrode would develop leaks around the metals. However, experiments with the NaOH solutions as well as characterization of the tips before and after extended exposure to concentrated NaOH solutions did not show any behavior that suggested the development of leaks, although there appeared to be considerable roughening of the electrode on continuous cycling in strongly alkaline solutions (Figure 1). A Pt disk electrode (diameter of 2.1 mm), sealed in soft glass, was used as the collector or substrate in SECM experiments and was employed as a working electrode for some electrochemical measurements. Prior to each experiment, the surfaces of Pt UMEs and Pt disk electrodes were polished with 0.3  $\mu\text{m}$  alumina and then cycled in Ar-saturated NaOH solution at a scan rate of 50 mV/s between the onset potentials of hydrogen and oxygen evolution reactions until reproducible cyclic voltammograms were obtained. The final potential was stopped at the onset potential of hydrogen evolution.

## Results and Discussion

### Steady-State Behavior of ORR in Aqueous NaOH Solutions.

Figure 1 shows the typical CV curve of a Pt UME in Ar-saturated 10 M NaOH aqueous solution at a scan rate of 50 mV/s. From the CV of the Pt UME, the hydrogen adsorption/desorption peaks and oxidation/reduction peaks of the Pt surface

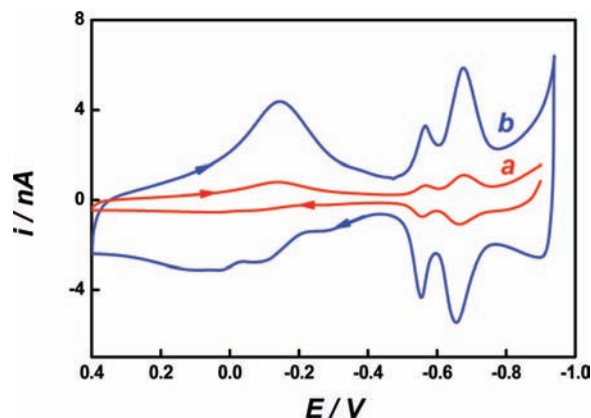


**Figure 1.** Typical CV curve of Pt UME (disk diameter, 25  $\mu\text{m}$ ) in Ar-saturated 10 M NaOH at 296 K; scan rate, 50 mV/s. Pt UME (a) newly polished (red curve) or (b) multicycled between hydrogen and oxygen evolution for 50 min (blue curve). Arrows indicate scan direction.

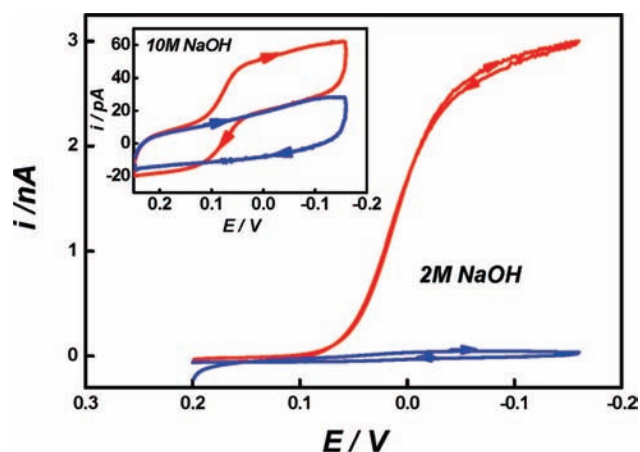


**Figure 2.** Steady-state CVs of Pt UME in 2 and 10 M NaOH; scan rate, 1 mV/s.  $O_2$ -saturated (red lines) and blank Ar-saturated (blue lines).

are clearly seen. The evolution of bulk hydrogen at  $-0.9$  V is at the position expected for a pH  $\sim 15$  solution.

According to the calculated area of the hydrogen adsorption/desorption peaks, using a value of 210  $\mu\text{C}/\text{cm}^2$ , the roughness factor of the Pt UME increased from 2.1 to 9.5 with continuous scanning over a period of about 50 min. The CVs of the same Pt UME in other Ar-saturated NaOH solutions were very similar to that in 10 M NaOH, with a small shift in potential for the waves at lower or higher pH. Steady-state CVs carried out in  $O_2$ -saturated and Ar-saturated 2 and 10 M NaOH solutions with a Pt UME are shown in Figure 2. When corrected for charging current, they show the expected classical S-shaped curves. Curves for other NaOH concentrations were similar to these. The relatively large contribution from charging current results from the small  $O_2$  solubility and diffusion coefficient, as discussed below, greatly diminishing the faradaic current for the ORR and the increased capacitance because of electrode roughening.

The difference between the apparent limiting steady-state currents ( $i_{ss,app}$ ) in the  $O_2$ -saturated solution and the blank Ar-saturated solution was used to obtain the limiting current for the ORR in the corresponding NaOH solution. The measure  $i_{ss}$  values are summarized in Table 1.

The results indicated that  $i_{ss}$  for the ORR decreased monotonically with increasing concentration of NaOH, because of increasing viscosity and decreasing  $O_2$  concentration. To obtain

(23) Singh, P. S.; Evans, D. H. *J. Phys. Chem. B* **2006**, *110*, 637.

(24) Andrieux, C. P.; Hapiot, P.; Saveant, J.-M. *J. Am. Chem. Soc.* **1987**, *109*, 3768.

(25) Denuault, G.; Mirkin, M. V.; Bard, A. J. *J. Electroanal. Chem. Interfacial. Electrochem.* **1991**, *308*, 27.

(26) See for example: (a) *Scanning Electrochemical Microscopy*; Bard, A. J., Mirkin, M. V., Eds.; Marcel Dekker: New York, 2001. (b) Bard, A. J.; Denuault, G.; Lee, C.; Mandler, D.; Wipe, D. O. *Acc. Chem. Res.* **1990**, *23*, 357.

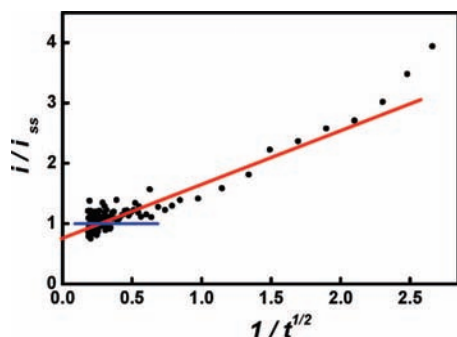


**Figure 3.**  $i/i_{ss}$  vs  $t^{-1/2}$  curve in 10 M NaOH. The potential was stepped to  $-0.1$  V. Dots are experimental data; red and blue lines indicate simulated results of transient and steady-state currents, where  $i_{ss} = 32$  pA.

**Table 1.** Effect of NaOH Solution Concentration ( $C_{\text{NaOH}}$ ) on Steady-State Current of ORR ( $i_{ss}$ )

	$C_{\text{NaOH}}$ (M)						
	1	2	4	6	8	10	12
$i_{ss}$ (nA)	15	2.8	0.94	0.32	0.092	0.032	0.013

the solubility of O<sub>2</sub> in the NaOH solutions employed from the steady-state tip current,

$$i_{ss} = 4anFD_{\text{O}_2}C_{\text{O}_2} \quad (2)$$

one needs to determine the diffusion coefficient of O<sub>2</sub> ( $D_{\text{O}_2}$ ) and the number of electrons,  $n$ , involved in the mass-transfer reaction in each NaOH solution.

**Diffusion Coefficient of Oxygen ( $D_{\text{O}_2}$ ) in NaOH.** One can measure the diffusion coefficient of an electroactive species without knowing its concentration and the number of electrons,  $n$ , involved by measuring both transient and steady-state currents in the diffusion-controlled regime at an UME.<sup>25,27</sup> The normalized current  $i/i_{ss} \sim t^{-1/2}$  relationship shown in eq 3 is a good approximation for the time range studied:<sup>25</sup>

$$\frac{i}{i_{ss}} = 0.7854 + 0.8862 \frac{a}{2\sqrt{Dt}} + \dots \quad (3)$$

In eq 3,  $a$  is the radius of the Pt UME and  $t$  is the measurement time. These  $i-t$  curves were obtained in O<sub>2</sub>-saturated NaOH solutions, correcting for background in Ar-saturated NaOH. Because the potential range of the ORR overlaps that of electroreduction of adsorbed oxygen species on the Pt surface, the  $i-t$  response acquired from Ar-saturated solution was used as the baseline for correction for the background contribution of adsorbed oxygen species on the Pt surface. The  $i/i_{ss}$  vs  $t^{-1/2}$  plots, which were obtained for each NaOH solution, can be used to evaluate the diffusion current of the O<sub>2</sub> molecule from the slope of the line. A representative  $i/i_{ss}$  vs  $t^{-1/2}$  curve in 10 M NaOH is shown in Figure 3.

The rapidly ascending portion of the  $i/i_{ss}$  vs  $t^{-1/2}$  curve at very short times can be attributed mainly to double-layer charging. The  $D_{\text{O}_2}$  values obtained from eq 3 in different NaOH solutions are listed in Table 2.

According to the Stokes–Einstein equation,

$$D = \frac{kT}{6\pi\eta r} \quad (4)$$

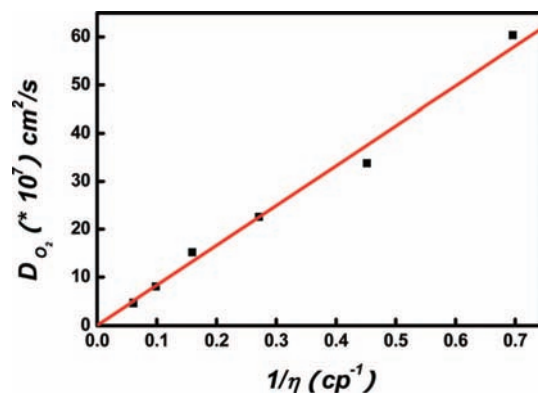


**Figure 4.** Plots of the diffusion coefficient,  $D_{\text{O}_2}$ , as a function of the reciprocal viscosity,  $1/\eta$ , for O<sub>2</sub> in 2–12 M NaOH solutions at 296 K based on UME measurements (e.g., Figure 3).

**Table 2.** Effect of Solution Concentration ( $C_{\text{NaOH}}$ ) on Diffusion Coefficient ( $D$ )

	$C_{\text{NaOH}}$ (M)						
	1	2	4	6	8	10	12
$D$ ( $\times 10^7$ cm <sup>2</sup> /s)	190	60.4	33.8	22.6	15.2	8.08	4.7

where  $k$  is the Boltzmann constant,  $T$  is the absolute temperature,  $\eta$  is the viscosity of the NaOH solution,<sup>28</sup> and  $r$  is the radius of the O<sub>2</sub> molecule (assumed spherical). The  $D_{\text{O}_2}$  vs  $1/\eta$  plot in Figure 4 shows a linear relationship between  $D_{\text{O}_2}$  and  $1/\eta$  with an intercept of zero when the NaOH concentration is  $\geq 2$  M; however,  $D_{\text{O}_2}$  in 1 M NaOH deviates considerably from this line. These results indicate that the radius of the dissolved O<sub>2</sub> molecule is constant and is independent of NaOH concentration, at about 2.8 Å in the NaOH concentration range from 2 to 12 M. This result suggests that the O<sub>2</sub> molecule is not highly hydrated in the NaOH solutions studied. The weak interaction between H<sub>2</sub>O molecules and dissolved O<sub>2</sub> probably leads to the low solubility of oxygen in these solutions. In addition, by comparing our results with those reported previously,<sup>29,30</sup> we conclude that the pure diffusion of electroactive species could still be described very accurately by the Stokes–Einstein equation over the concentration range of electrolytes studied. Moreover, the diffusion behavior of the electroactive species is mainly affected by the viscosity of solutions and is not related to the nature of the solutions (either electrolytes or nonelectrolytes).<sup>29,30</sup> Furthermore,  $D_{\text{O}_2}$  is mainly controlled by the viscosity of the solution and the size of electroactive species but is not affected by the detailed electrode reaction mechanism.

#### Solubility of Oxygen ( $C_{\text{O}_2}$ ) in Aqueous Solution of NaOH.

From  $D_{\text{O}_2}$  obtained in different NaOH solutions,  $C_{\text{O}_2}$  in each NaOH solution can easily be evaluated from the steady-state diffusion current at the UME, eq 2, with  $n$  assumed to be 1 or 2, for reduction to superoxide or peroxide, respectively. At the same time,  $C_{\text{O}_2}$  acquired by nonelectrochemical techniques, either experimental or theoretical,<sup>31,32</sup> can be used. Figure 5 compares results from this work with  $n = 1$  or 2 (where  $n$  is the number of electrons transferred) with literature data (triangles).

(28) Weast, R. C.; Astle, M. J.; Beyer, W. H. *CRC Handbook of Chemistry and Physics*, 67th ed.; CRC Press: Boca Raton, FL, 1986–1987; D-257.

(29) Zhang, X.; Leddy, J.; Bard, A. J. *J. Am. Chem. Soc.* **1985**, *107*, 3719.

(30) Zhang, X.; Yang, H. J.; Bard, A. J. *J. Am. Chem. Soc.* **1987**, *109*, 1916.

(31) Tromans, D. *Ind. Eng. Chem. Res.* **2000**, *39*, 805.

(32) Tromans, D. *Hydrometallurgy* **1998**, *50*, 279, and references therein.

(27) Bard, A. J.; Faulkner, L. R. *Electrochemical Methods: Fundamentals and Applications*, 2nd ed.; John Wiley and Sons: New York, 2001; Chap. 5.



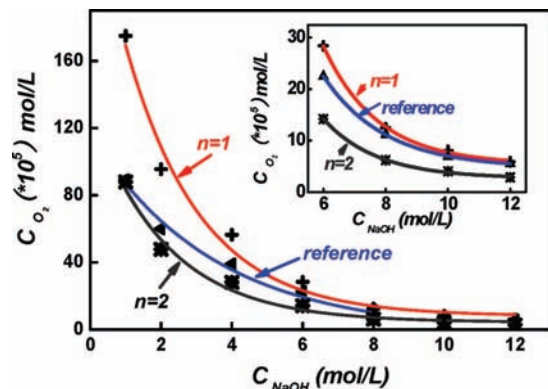


**Figure 5.**  $C_{O_2}$  as a function of NaOH concentration. Red and black lines are experimental data calculated from  $D_{O_2}$  assuming  $n = 1$  or  $2$ , respectively. Triangles are taken from the literature.

With either assumption,  $C_{O_2}$  clearly decreases strongly with an increase in the NaOH concentration. From a comparison with the results reported previously,<sup>31,32</sup> shown as the blue line in Figure 5, the conclusion can be drawn that  $C_{O_2}$  acquired by nonelectrochemical methods and a thermodynamic model agrees better with  $C_{O_2}$  obtained on the basis of eq 2 with the assumption that  $n = 2$  in more dilute NaOH solutions, while that with  $n = 1$  is closer at the higher NaOH concentrations. This result suggests that the ORR proceeds via an electrochemical–chemical–electrochemical process with a one-electron transfer reaction producing  $O_2^{\cdot-}$ , which reacts with water in a protonation reaction, followed by another one-electron transfer to produce  $HO_2^-$ . In dilute NaOH solutions, protonation is fast and an overall two-electron reduction takes place. In concentrated NaOH there is little protonation and the one-electron transfer reaction to produce  $O_2^{\cdot-}$  occurs.

The absolute amount of  $O_2^{\cdot-}$  formed is not only controlled by the fraction of the 1e reaction that occurs during the reduction, but it is also limited by the small solubility of  $O_2$  in concentrated NaOH solutions. In contrast, in aprotic solutions, owing to the higher solubility of oxygen and weak proton conditions, the rate of disproportionation of  $O_2^{\cdot-}$  is slow, and the electrochemical behavior of the  $O_2/O_2^{\cdot-}$  couple can be readily examined. However, it is difficult to achieve high solubility of oxygen under the weak proton conditions of concentrated NaOH solutions, so it is quite challenging to explore the electrochemical behavior of  $O_2/O_2^{\cdot-}$  in aqueous solutions.

**SECM Study on ORR in 10 M NaOH Solution.** Since the low  $O_2$  solubility makes CV studies in viscous 10 M NaOH difficult, the  $O_2/O_2^{\cdot-}$  reaction was studied by SECM, where measurements in the steady-state mode can be made with a smaller contribution from capacitive and surface background currents. Oxygen reduction was carried out at the tip, and  $O_2^{\cdot-}$  oxidation occurred at the substrate in the feedback mode of SECM shown in Figure 6.

A series of approach curves at different substrate potentials were obtained, as shown in Figure 7. The SECM approach curves reflect the relationship between the normalized distance,  $d/a$ , and normalized tip current,  $i/i_{T,\infty}$ , where  $d$  is the distance between tip and substrate,  $i$  is the instantaneous tip current at any distance between tip and substrate, and  $i_{T,\infty}$  is the current when the tip is far from the substrate. When the tip is far from the substrate and held at a potential of  $-0.15$  V, where the ORR occurs at a diffusion-controlled rate, the measured  $i_{T,\infty}$  is the same as the limiting  $i_{ss}$  described in the voltammetry experi-

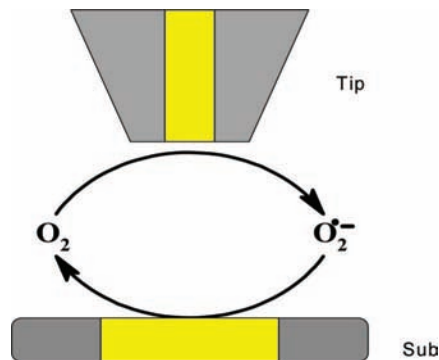


**Figure 6.** Feedback mode of SECM used in the study of ORR in NaOH solution. Gray, glass wall; yellow, Pt.

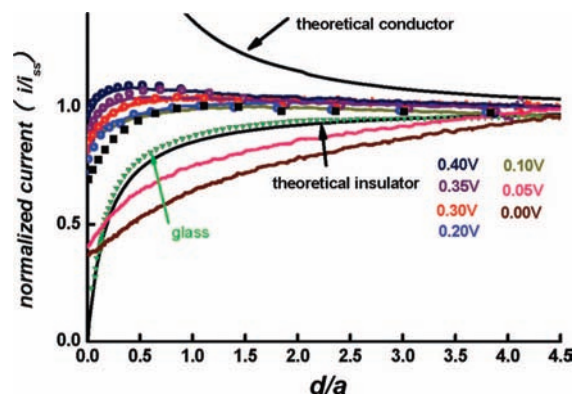


**Figure 7.** SECM approach curves acquired in  $O_2$ -saturated 10 M NaOH solution. The Pt tip (Pt UME) potential was held at  $-0.12$  V, corresponding to the diffusion-limited current for  $O_2$  reduction; lines are the normalized tip current acquired at different Pt substrate potentials as indicated in the figure. Solid lines are experimental data and hollow circles are theoretical curves at a Pt substrate with the rate constants,  $k$ , shown in Figure 8 corresponding to  $E_s = 0.4, 0.35, 0.3, 0.2,$  and  $0.1$  V. Shielding effects were shown at  $E_s = 0.05$  and  $0.0$  V, respectively. Negative feedback was acquired at a glass (insulator) substrate (triangles-dotted line). Approach speed,  $0.2 \mu\text{m/s}$ .

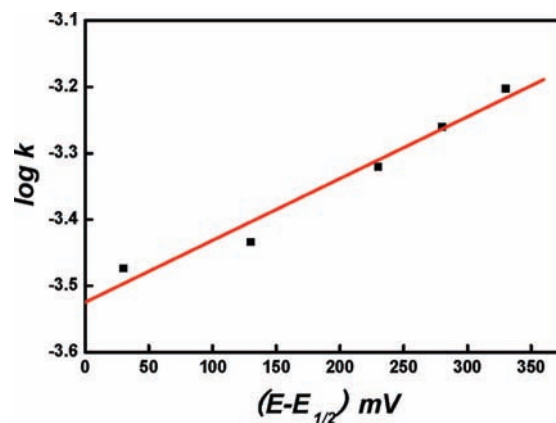


**Figure 8.** Plot of  $\log k \sim (E - E_{1/2})$  for  $O_2/O_2^{\cdot-}$  couple on platinum in 10 M NaOH from fit of SECM approach curves in Figure 7.

ments. The approach to a glass substrate (triangles-dotted line) follows the usual negative feedback.<sup>26</sup> Here, as the Pt UME tip gradually approaches the substrate, the narrow separation between tip and substrate blocks oxygen diffusion into the gap, causing a decrease in the current compared to  $i_{T,\infty}$ . When Pt was used as the substrate, the behavior was more complex. With the Pt substrate at the less positive potentials, negative of the

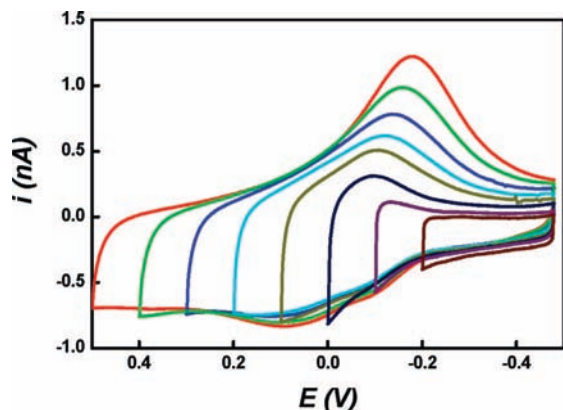


**Figure 9.** Typical CV curve group of Pt UME (disk diameter, 25  $\mu\text{m}$ ) in Ar-saturated 10 M NaOH at 296 K; scan rate, 50 mV/s. The initial potential is  $-0.4$  V, and reverse potential from  $-0.2$  to 0.5 V.

half-wave potential of the ORR (see inset of Figure 2), where the ORR occurs not only on the tip but also on the Pt substrate, there was evidence of shielding at the longer distances.<sup>33</sup> In this case, the oxygen in the NaOH solution near the Pt substrate was also reduced, so compared to the glass substrate, there is less oxygen in the gap. When the potential of the Pt substrate was kept at more positive values, positive of the half-wave potential, O<sub>2</sub><sup>•−</sup> formed on the Pt UME could be oxidized back to O<sub>2</sub> on the surface of the Pt substrate at a rate determined by the electron-transfer kinetics there. This results in the observed positive feedback approach curves.

These approach curves can be employed to obtain information about the kinetics of the ORR reaction in 10 M NaOH, based on procedures reported previously.<sup>34</sup> Here one can obtain  $k$ , the rate constant of the heterogeneous electron-transfer reaction for the anodic reaction (cm/s) as a function of substrate potential,  $E_s$ .



The anodic rate constant,  $k_b$ , and the anodic charge-transfer coefficient,  $1 - \alpha$ , are defined in the usual way:

$$k_b = k^\circ \exp\left[\frac{(1 - \alpha)F}{RT}(E - E^0)\right]$$

The results are shown in Figure 8. The half-wave potential,  $E_{1/2} = 0.070$  V, of the S-shaped steady-state O<sub>2</sub> reduction CV curves (inset of Figure 2) was taken as the equilibrium potential ( $E_{\text{eq}}$ ) of the O<sub>2</sub>/O<sub>2</sub><sup>•−</sup> couple for the calculation of overpotential ( $E - E_{\text{eq}}$ ). The diffusion coefficient of O<sub>2</sub><sup>•−</sup> was taken to be equal to that of O<sub>2</sub>,  $8.08 \times 10^{-7}$  cm<sup>2</sup>/s. A plot of  $\log k$  vs ( $E - E_{1/2}$ ) is shown in Figure 8.

The intercept of the  $\log k$  vs ( $E - E_{1/2}$ ) line yields an apparent rate constant,  $k^\circ$ , of  $2.6 \times 10^{-4}$  cm/s. This puts the reaction in the regime usually considered as quasi-reversible. The slope of the plot is  $0.93 \text{ V}^{-1}$  and yields an apparent  $(1 - \alpha)$  of 0.08. The  $k^\circ$  value is quite small for what appears to be a simple 1e transfer, so it is worthwhile to consider the factors that might

make this so. Note that in a study of this reaction at a methylphenyl-modified carbon electrode in 1 M KOH,  $k^\circ = 3 \times 10^{-3}$  cm/s and  $\alpha = 0.5$  were reported.<sup>14</sup> A small  $k^\circ$  is also consistent with values obtained in aprotic media.<sup>35</sup> The rate could be even smaller in 10 M NaOH for several reasons. The solution viscosity of this medium is about an order of magnitude higher than that for dilute NaOH solutions (and even more compared to 1 M KOH). It has been reported for other outer-sphere 1e systems that the heterogeneous reaction rate decreased significantly with increasing viscosity of the solution.<sup>29,30</sup> However, besides the effect of solution properties, the SECM approach curves show an unusually weak dependence of the tip feedback current on the substrate potential, as reflected by the small  $(1 - \alpha)$  value. This suggests that an oxide film could be formed on the surface of the Pt substrate as the potential is made more positive. Oxide films on Pt are known to decrease electron-transfer rates for many systems. This is confirmed by the CV results shown in Figure 9, where the amount of Pt oxide reduced is a function of the positive potential excursion. One sees growth of the oxide film beginning at  $-0.1$  V. Thus, the feedback current is controlled by two factors: an increase in the rate of oxidation of O<sub>2</sub><sup>•−</sup> by the increasing substrate potential, countered by the growth of oxide film. The two factors nearly counterbalance, leading to the weak correlation between tip feedback current and overall substrate potential and the unusually low apparent  $(1 - \alpha)$  value.

## Conclusions

An UME has been used for the accurate measurement of important parameters such as the diffusion coefficient of O<sub>2</sub> without requiring knowledge of its concentration or the mechanism of its electrochemical reduction. The diffusion coefficient and solubility of oxygen decrease significantly and the number of electrons involved in the overall ORR changes from 2 to 1 with an increase in the NaOH concentration. The formation of solution-phase O<sub>2</sub><sup>•−</sup> is probably the first elementary step in the overall process of ORR, followed by protonation by water and a second electron-transfer step to form peroxide. Scanning electrochemical microscopy was employed in 10 M NaOH to study the O<sub>2</sub>/O<sub>2</sub><sup>•−</sup> system. By fitting the SECM approach curves for O<sub>2</sub> reduced at a Pt tip and O<sub>2</sub><sup>•−</sup> oxidized at a Pt substrate, the heterogeneous rate constant for the reaction could be measured. The relatively small value for this quasi-reversible reaction suggests appreciable viscosity and Pt oxide film effects.

**Acknowledgment.** This project was supported by grants from the Robert A. Welch Foundation (F-0021) and the National Science Foundation (CHE 0451494). C.Z. thanks the Foundation of National Key Research and Development Program (Grant No. 2002CB211800) and the National Key Program for Basic Research of China (2001CCA05000), Teaching & Research Fund of Beijing Institute of Technology (05120404) and Excellent Young Scholars Research Fund of Beijing Institute of Technology (000Y05-19) of China, and the National Scholarship Fund of China Scholarship Council (2005A09007) for support. Joaquin R. Lopez is also gratefully acknowledged for helpful discussions.

JA8064254

(33) See, for example: Zoski, C. G.; Aguilar, J. C.; Bard, A. J. *Anal. Chem.* **2003**, *75*, 2959.

(34) Bard, A. J.; Mirkin, M. V.; Unwin, P. R.; Wipf, D. O. *J. Phys. Chem.* **1992**, *96*, 1861.

(35) Bollo, S.; Jara-Ulloa, P.; Finger, S.; Núñez-Vergara, L. J.; Squella, J. A. *J. Electroanal. Chem.* **2005**, *577*, 235.